

# Weld bead formation by a 10 kW class high power fiber laser on 16 mm thickness carbon steel plate<sup>†</sup>

SHIN Minhyo \*and NAKATA Kazuhiro \*\*

## Abstract

*In this study, weld characteristics of high power fiber laser welding with a maximum output of 10 kW on thick carbon steel plate were evaluated. Both bead-on-plate and butt joint welding were conducted on SS400 carbon plate of 16 mm thickness under various welding parameters. Acceptable weld profiles with a deep and narrow weld bead and without apparent defects such as undercut and melt-through can be obtained by single pass process at the optimized welding parameters. Porosity was observed in both cases of partially-and fully-penetrated weld beads. From residual gas analysis results of the porosity, trapping of Ar shielding gas was a main reason for porosity formation in the partially-penetrated weld bead, whereas trapping of infiltrated N<sub>2</sub> gas from Air atmosphere through keyhole opened in the weld pool on the back side and resultant CO gas were major causes in the fully-penetrated weld bead.*

**KEY WORDS:** (High power fiber laser), (Weld characteristics), (SS400 carbon plate), (Porosity).

## 1. Introduction

Laser welding has many advantages such as narrow weld width, narrow HAZ, deep penetrations and small heat distortion [1].

Among the variety of laser beams, the high power fiber laser, which was developed recently, has high energy efficiency, high beam quality at high power range compared to a conventional type of laser. Moreover fiber laser has wave length of 1070 nm, which allows transmission in flexible fibers [2-3] and minimizes the laser absorption by laser induced plasma [4].

Thus, the fiber laser is considered as a new welding heat source in fields where the application of conventional arc is difficult such as in high speed welding of thick plate joint.

However, because of its short study history, research on welding characteristics by high power fiber laser in high speed welding, especially on thick steel plate, is limited [5] and the base data is not sufficient for industrial application up to now.

Therefore, in this study, welding characteristics are evaluated using a high power fiber laser in SS400 of 16 mm thickness. To obtain sound 1 pass fully-penetrated welding beads, appropriate welding parameters were evaluated.

## 2. Materials and experimental procedure

SS400 mild steel plate of 16 mm thickness was used and its chemical composition is shown in **Table 1**. The oxidation layer of the plate on front side was removed by a sand blaster. A schematic diagram of the laser welding system is shown in **Fig. 1**. Laser beam is irradiated vertically on the plate surface. 100 % Ar was used as shielding gas and it was provided through a nozzle of 10 mm in diameter from the front side to the weld zone. A 10 kW class fiber laser (IPG) was used with a fiber diameter of 100 $\mu$ m and focus length of 250 mm. Focused beam diameter was 200 $\mu$ m and constant. Laser beam size on the plate surface was changed by changing the defocused distance as shown in **Fig. 2**. In order to evaluate welding bead characteristics, welding bead appearance and cross section were observed by an optical microscope. Cross section of the welds was prepared by cutting with micro cutter and polished, then etched by 2% nital to reveal the microstructure. In order to define the mechanisms of porosity formation, x-ray radiograph and gas analysis were performed. Residual gas in the porosity was analyzed by Anelva AGS-7000 Quadruple-pole Mass Analysis Meter, which can measure the gas released from the opened porosity by drilling in a vacuum condition. The parameters of the gas analysis are shown in **Table 2**.

<sup>†</sup> Received on June 11, 2010

\* Graduate Student

\*\* Professor

Transactions of JWRI is published by Joining and Welding Research Institute, Osaka University, Ibaraki, Osaka 567-0047, Japan

## Weld bead formation by a 10 kW class high power fiber laser on 16 mm thickness carbon steel plate

### 3. Results and discussion

#### 3.1 Deep penetration at high laser power

Figure 3 shows cross sections of weld beads at various conditions of laser power changed from 3 kW to 10 kW and welding speed from 0.5 m/min to 10 m/min. Focal point of the laser beam was fixed on the plate surface. With the increase of welding speed, weld beads with very narrow width and deep depth were obtained. Especially at a laser power of 10 kW and welding speed of 10 m/min, a

needle-like weld bead with the bead width less than 1 mm and the depth over than 8 mm was formed. On the other hand, at 10 kW of laser power and 0.5 m/min of welding speed, 1 pass fully-penetrated weld bead was obtained.

However, underfilling and melt-through occurred in the front side and the back side respectively. It is believed that high heat input makes a wide weld bead at the bottom side which can not sustain the molten metal, and thus underfilling and melt-through occurs.

**Table 1** Chemical composition of SS400.

Material	Elements (mass%)										
	C	Si	Mn	P	S	Cu	Ni	Cr	Mo	Al	Fe
SS400	0.15	<0.01	0.81	0.013	<0.005	0.09	0.02	0.06	<0.01	0.025	Bal.

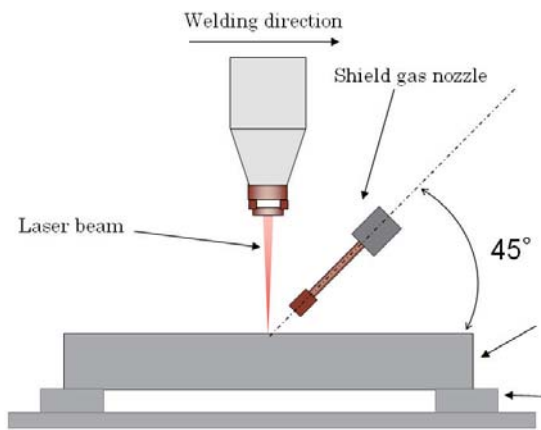


**Fig. 1** Schematic of the experimental setup for the fiber laser welding.

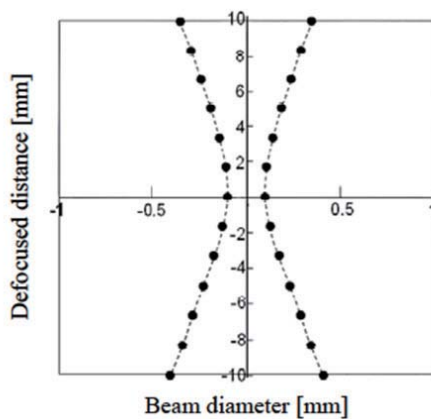


**Fig. 2** The fiber laser beam profile with defocused distance (fd).

**Table 2** Parameters of quadruple-pole mass analysis meter for gas analysis.

Ionisation energy	70 eV
CEM voltage*	-1400 V
Mass number range	2-100
Scanning time	0.52 s/scan
Beginning vacuum degree	About $5 \times 10^{-6}$ Pa
Cutting-tool	2 $\phi$ drill

\*CEM refers to channel electron multiplier.

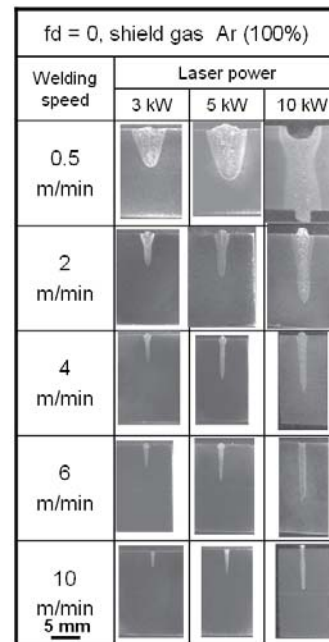


**Fig. 3** Cross sections of fiber laser weld bead with different laser powers and welding.

**3.2 Effect of defocused distance on weld bead formation**

The effect of defocused distance on weld bead formation is shown in Fig. 4. Deeper penetrations were obtained at defocused distances (fd) ranging from -10 mm to -4 mm. At larger or smaller fd, the penetration depth was likely to decrease in each case. Based on above results, setting the focal point at the inside of the plate is better than just on the plate surface and above the plate. Figure 5 shows the effect of fd on the depth and the width of weld bead and their ratio of depth to width. At -4 mm to -10 mm of fd, the depth/width ratio showed the highest value of about 6 to 8, which is similar to typical deep penetration weld bead made by electron beam welding.

Figure 6 shows the effect of welding speed on the weld bead formation at 10 kW of laser power, when the fd was set at -7 mm, the middle of the plate thickness. At the welding speed of 0.5 m/min, 1 pass sound fully-penetrated bead without melt-through and underfill can be obtained. Narrow width of weld bead is important to protect the melt-through of molten metal in fully-penetrated condition. At higher welding speed, penetration depth decreased remarkably with an increase of welding speed. In addition at 0.5 m/min the shape of cross section of weld bead was almost same as the laser beam profile. It seems to one of the features of high power laser.

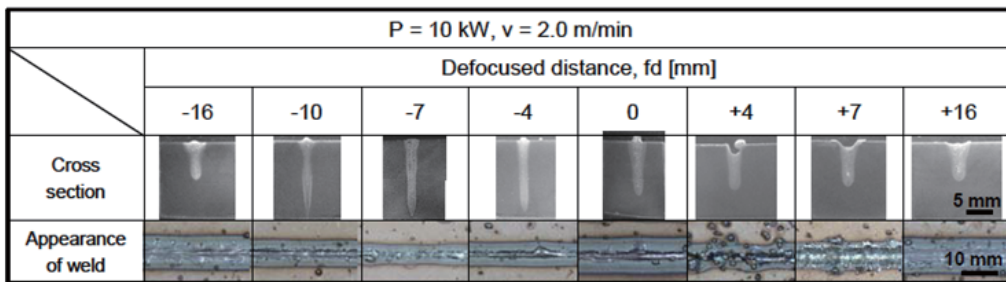


Fig. 4 Effect of defocused distance fd on the weld bead formation in fiber laser welding of 16 mm thick plate of SS400.

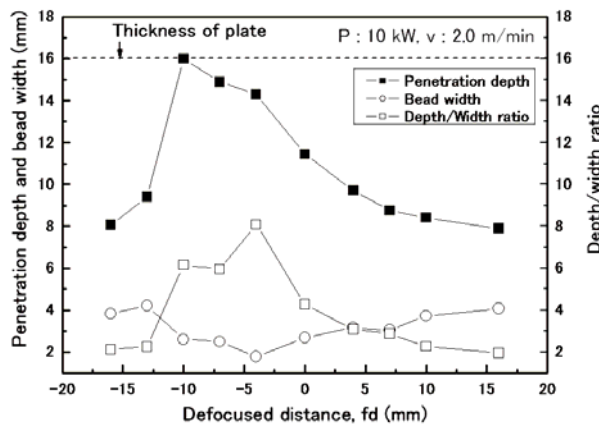


Fig. 5 Relationship between shapes of the fiber laser welds and defocused distance fd at constant laser power 10 kW and welding speed 2.0 m/min for 16 mm thick plate of SS400.

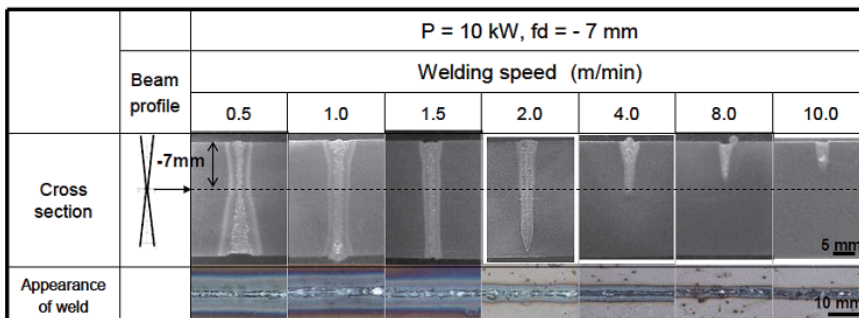


Fig. 6 Welding speed range for single pass fully-penetrated weld bead at constant laser power 10kW, and defocused distance fd - 7 mm for 16 mm thick plate of SS400.

## Weld bead formation by a 10 kW class high power fiber laser on 16 mm thickness carbon steel plate

### 3.3 Porosity

In finely focused high power laser, porosity is formed easily by violence of molten metal flow in the weld metal [6]. In this study, under the broad welding parameters range porosity was observed as shown in Fig. 4 and Fig. 6. Since porosity reduces the mechanical property of the laser weld bead, the reduction mechanism of porosity has to be revealed.

**Figure 7** shows the appearance, cross section and x-ray radiograph of typical partially-penetrated weld bead with the depth of about 15 mm obtained at 10 kW, 2.0 m/min and fd - 7 mm. The black arrows indicate the location of porosity on x-ray radiograph. **Table 3** shows the analysis results of the residual gas in the porosity. Two porosities were selected for analyzing. Analysis result shows that most of the residual gas detected is Ar gas, which occupies 98.7% and 97.0 % with small amount of H<sub>2</sub> and N<sub>2</sub> (or CO) gas. These results apparently show that trapping of shielding gas in the fusion zone is the main reason for porosity formation as well as small amount of air, which causes N<sub>2</sub>(or CO) and H<sub>2</sub> originated from H<sub>2</sub>O vapor in the air. It is generally known that the shielding gas trapping during laser weld is caused by the instability of keyhole and this makes porosity.

On the other hand, **Fig.8** shows the appearance of cross section and x-ray-radiograph of fully-penetrated weld bead which was obtained at welding speed 1.5 m/min and other welding parameters are the same as in Fig.7. X-ray-radiographs were obtained from different directions, one is from the top side of the weld bead and the other is

from the side view, which was obtained by using the specimen with narrow width along the weld bead cut out of the welded joint. The top and bottom of x-ray radiograph in the side view correspond to the top and bottom of the weld bead, respectively.

Porosity in fully-penetrated weld bead was indicated by white arrows in the front view. In addition, black spots with irregular shape in the side view also indicate porosity. Residual gas composition was quite different with that of the porosity in the partially-penetrated weld bead, namely as shown in **Table 3**, major gas of porosity was N<sub>2</sub> (or CO), up to 91% to 98 % and small amount of Ar and H<sub>2</sub> was also detected. From these results, it is estimated that in this case, the bottom bead surface was not shielded, thus air can infiltrate into fusion zone through the open keyhole on the bottom bead surface and be trapped as porosity, so containing N<sub>2</sub> as the major gas, and Ar and H<sub>2</sub> as minor gas as originated from air. CO gas is possible to be formed from the reaction between carbon of the material and oxygen in air.

In conventional laser welding with CO<sub>2</sub> and YAG lasers, porosity is likely to form in a partially-penetrated weld bead with a deep penetration by a trapping shielding gas; such as Ar due to the instability of a keyhole during welding [7-8]. Therefore, weld bead porosity is much less in a fully-penetrated weld bead. On the other hand, in a fiber laser welding porosity was formed even in the fully-penetrated weld bead with deep penetration for very thick plate.

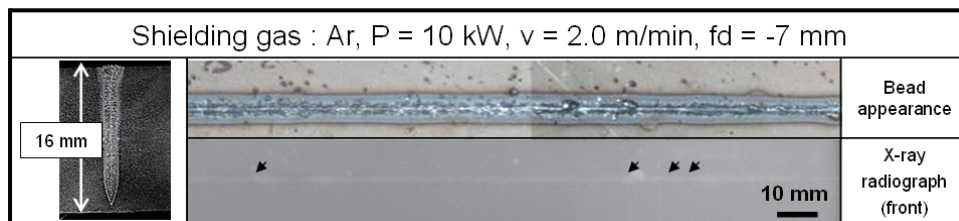


**Fig. 7** Bead appearance and x-ray radiography inspection result of the partially-penetrated weld bead for 16 mm thick plate of SS400.

**Table 3** Residual gas composition and content in the porosity of the weld beads.

Shielding gas	Partially-penetrated		Fully-penetrated	
	WM1	WM 2	WM 1	WM 2
Ar				
H <sub>2</sub> (M/Z 2*)	-	2.0	3.9	-
N <sub>2</sub> , CO (M/Z 28)	1.3	1.0	91.3	97.5
Ar (M/Z 40)	98.7	97.0	4.8	2.5
CO <sub>2</sub> (M/Z 44)	-	-	-	-
Total	100.0	100.0	100.0	100.0
Gas volume, mL	4X10 <sup>-5</sup>	3X10 <sup>-5</sup>	6X10 <sup>-5</sup>	7X10 <sup>-5</sup>

\*M/Z refers to mass number.

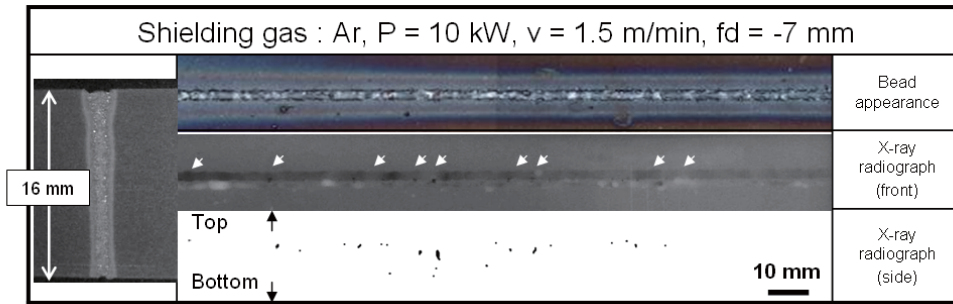


**Fig. 8** Bead appearance and x-ray radiography inspection result of the fully-penetrated weld bead for 16 mm thick plate of SS400.

**3.5 Root gap bridging ability**

From the standing point of practical application of laser welding, it is well known that a fine laser beam is not always beneficial for making a sound welded joint.

**Figure 9** shows the root gap bridging ability of fiber laser welding of a butt joint with different root gaps. Weld bead formation was only possible up to 0.2 mm of root gap irrespective of fd, which is almost the same for the focused

beam diameter. Over 0.5 mm of root gap, bridging of weld bead was difficult. To overcome this drawback, larger diameters of laser beam can be select at the sacrifice of the deep penetration. In addition filler wire addition or hybrid welding with MIG · MAG Arc welding may be expected.

		P = 10 kW, v = 1.5 m/min, Ar 100%			
		Root gap [mm]			
fd		0.1	0.2	0.5	0.7
0 mm				-	
-7 mm				5 mm	
-13 mm					

**Fig. 9** Effect of root gap width and defocused distance fd on the bead formation of high power fiber laser with the beam diameter of 0.2 mm at the focal point.

**4. Conclusions**

Weld bead formation of 10 kW fiber laser in 16 mm thick plate of SS400 has been studied. Following conclusive remark can be obtained.

- (1) Very narrow and deep penetrated weld beads with needle like shape were obtained by high power fiber laser welding.
- (2) The maximum penetration depth for a weld bead was obtained at the focal point of -10 mm to -4 mm below the plate surface.
- (3) Sound welds without underfill and melt-through can be

obtained at the focal point of -7 mm with below the plate surface 10 kW of laser power and 1.5 m/min of welding speed.

- (4) In partially-penetrated weld bead, porosity was caused by Ar shielding gas trapping in the keyhole, however, in full-penetrated weld bead, the major residual gas in porosity was N<sub>2</sub> (or CO) which came from air without gas shielding, and this suggested that porosity was caused by air trapping into the keyhole from the back surface of the weld bead.

## Weld bead formation by a 10 kW class high power fiber laser on 16 mm thickness carbon steel plate

### References

- 1) W. M. Steen : Laser material processing, Second edition, Springer, London, New York, (1998), pp.147-151.
- 2) L. Quintino, A. Costa, R. Miranda, D. Yapp, V. Kumar and C.J. Kong : Welding with high power fiber lasers-a preliminary study, Materials and design, 28(2007), pp.1231-1237.
- 3) Z. Liu, G. Xu and M. Kutsuna : Laser and laser-MAG hybrid welding of high strength steel using fiber laser and CO2 laser, Quarterly journal of the Japan welding society, 25-2(2007), pp.254-260.
- 4) Y. Kawahito, K. Kinoshita, N. Matsumoto, M. Mizutani and S. Katayama : High speed observation and spectroscopic analysis of laser-induced plume in high power fiber laser welding of stainless steel, Quarterly journal of the Japan welding society, 25-3(2007), pp.455-460
- 5) Y. Kawahito, K. Kinoshita, N. Matsumoto, M. Mizutani and S. Katayama : Interaction between laser beam and plasma/plume induced in welding of stainless steel with ultra-high power density fiber laser, Quarterly journal of the Japan welding society, 25-3(2007), pp.461-467
- 6) Y. Kawahito, M. Mizutani, and S. Katayama : Defect formation mechanism and reduction procedure in 10 kW high power fiber laser welding of stainless steel, Quarterly journal of the Japan welding society, 26-3(2008), pp.203-209
- 7) I. Kawaguchi, S. Tsukamoto, G. Arakane and H. Honda : Characteristics of high power CO2 laser welding and porosity suppression mechanism by nitrogen shield, Quarterly journal of the Japan welding society, 23-2(2005), pp.259-264
- 8) I. Kawaguchi, S. Tsukamoto, G. Arakane and K. Nakata : Formation mechanism of porosity in deep penetration laser welding, Quarterly journal of the Japan welding society, Volume 24-4(2006), pp.338-343